Journal of Magnetism and Magnetic Materials 324 (2012) 3029–3033

Contents lists available at SciVerse ScienceDirect

Journal of Magnetism and Magnetic Materials

journal homepage: www.elsevier.com/locate/jmmm

Magnetic properties of nanoscale crystalline maghemite obtained by a new synthetic route

L.A. Mercante [a], W.W.M. Melo [b], M. Granada [c], H.E. Troiani [c], W.A.A. Macedo [d], J.D. Ardison [d], M.G.F. Vaz [a], M.A. Novak [b,*]

[a] Instituto de Química, Universidade Federal Fluminense, Niterói, RJ, Brazil
[b] Instituto de Física, Universidade Federal do Rio de Janeiro, Rio de Janeiro, RJ, Brazil
[c] Centro Atómico Bariloche and Instituto Balseiro, Comisión Nacional de Energía Atómica, 8400 S.C. de Bariloche, RN, Argentina
[d] Laboratório de Física Aplicada, CDTN/CNEN, Belo Horizonte, MG, Brazil

ARTICLE INFO

Article history:
Received 27 August 2011
Received in revised form
19 April 2012
Available online 10 May 2012

Keywords:
Nanomagnetism
Magnetic material
Co-precipitation
Dipolar interaction

ABSTRACT

In this work we describe the synthesis and characterization of maghemite nanoparticles obtained by a new synthetic route. The material was synthesized using triethylamine as a coprecipitation agent in the presence of the organic ligand *N,N′*-bis(3,5-di-tert-butyl-catechol)-2,4-diaminotoluene (LCH_3). Mössbauer spectrum at 4 K shows typical hyperfine parameters of maghemite and Transmission Electron Microscopy images reveal that the nanoparticles have a mean diameter of 3.9 nm and a narrow size distribution. AC magnetic susceptibility in zero field presents an Arrhenius behavior with unreasonable relaxation parameters due to the strong influence of dipolar interaction. In contrast when the measurements are performed in a 1 kOe field, the effect of dipolar interactions becomes negligible and the obtained parameters are in good agreement with the static magnetic properties. The dynamic energy barrier obtained from the AC susceptibility results is larger than the expected from the average size observed by HRTEM results, evidencing the strong influence of the surface contribution to the anisotropy.

1. Introduction

The synthesis and characterization of magnetic nanoparticles is one of the most important aims in nanomagnetism, mainly due to many technological applications. The chemical and physical stability as well as intrinsic magnetic properties made nanocrystalline maghemite (γ-Fe_2O_3) an essential magnetic component for the magnetic storage media industry [1]. Moreover, this iron oxide and its close relative magnetite (Fe_3O_4) are the only magnetic materials approved for use in biomedical applications, including magnetic isolation and separation of labeled cells, magnetic drug and radioactive targeting, tumor treatment via hyperthermia and image-intensifying contrast agents for NMR imaging [2]. For technological applications, these oxides have to be produced by well-characterized, cost effective and controllable processes that afford functionalized nanoparticles of a certain size, morphology and narrow size distribution. There are many routes to produce stable colloidal dispersions of magnetic iron oxides either by physical or chemical methods [3]. In this work we describe the synthesis and characterization of maghemite nanoparticles obtained by the use of triethylamine as a coprecipitation agent in the presence of the organic ligand *N,N′*-bis(3,5-di-tert-butyl-catechol)-2,4-diaminotoluene (LCH_3), which proved to be a promising method to obtain small nanoparticles with a narrow size distribution.

2. Experimental

2.1. Synthesis

The ligand LCH_3 was synthesized using the same procedure as previously described [4]. Iron oxide nanoparticles were prepared by mixing 350 mg of iron(II) chloride to 500 mg of ligand LCH_3 in 25 mL of acetonitrile and heating the resulting mixture under reflux for three hours in the presence of 0.8 mL of triethylamine. The resulting solid was filtered, washed with acetonitrile and dissolved in 20 mL of ethyl ether. The resulting suspension was filtered yielding a light brown powder, which was washed with ether.

2.2. Characterization

The sample was characterized by XRD (X-ray diffraction), Mössbauer spectroscopy, TEM (Transmission Electron Microscopy), and magnetic susceptibility measurements. XRD measurement was performed using a Bruker D8 Advance diffractometer with

* Corresponding author. Tel.: +55 21 2562 7666.
E-mail address: mnovak@if.ufrj.br (M.A. Novak).

0304-8853
http://dx.doi.org/10.1016/j.jmmm.2012.04.049

Cu Kα radiation from 15° to 85° (2θ) at room temperature. The Mössbauer spectra were recorded in transmission geometry using a conventional spectrometer operating in constant acceleration mode. A ^{57}Co in Rh matrix was used as the radioactive source. The measurements were made without application of external magnetic field, at temperatures of 300 K and 4 K. The spectra were fitted using the program "NORMOS". Transmission electron microscopy (TEM) experiments were performed in a CM 200 Philips TEM equipped with an Ultra Twin objective lens, operating at 200 keV. The nanoparticles were deposited on a commercial copper grid covered with an ultrathin carbon film by immersion in a suspension of the nanoparticles in ethanol. Samples for magnetic measurements were prepared from a washed powder without addition of any surfactant or ligand, pressed inside a gelatin capsule. Zero Field Cooled (ZFC) and Field Cooled (FC) magnetization and hysteresis curves were measured using a Cryogenic SX600 superconducting quantum interference device (SQUID) magnetometer. AC susceptibilities were measured in a Quantum Design PPMS susceptometer.

3. Results and discussion

3.1. Synthesis

In coprecipitation methods described in the literature, when $FeCl_2$ or a mixture of $FeCl_2$/$FeCl_3$ is used in the synthesis, an oxidizing agent is necessary to obtain maghemite nanoparticles [5–8]. In our case, maghemite was synthesized starting from a Fe(II) salt in the presence of the ligand LCH_3 and triethylamine. Although the coprecipitation method is largely used in the synthesis of nanoparticles, this is the first time that triethylamine was used as a coprecipitation agent. Actually, this base is used to deprotonate this kind of ligand in the synthesis of coordination compounds [9]. The fact that the ligand can exist in five oxidation states and the formation of these complexes involves oxi–reduction reactions might be important in the formation of the maghemite nanoparticles. Although further detailed studies are needed to understand the mechanism by which the formation of nanoparticles occurs, the presence of the ligand LCH_3 seems to have an important role in the size limitation of the maghemite nanoparticles obtained in this work.

3.2. Characterization

X-ray powder diffraction patterns indicate the formation of nanocrystalline spinel phase due to either Fe_3O_4 or γ-Fe_2O_3 (Fig. 1). A mean diameter of 3.0 nm was estimated from the width of the reflections from the (311) planes (2θ=35.8°) using Scherrer's equation.

Fig. 2 shows the Mössbauer spectra obtained at 300 and 4 K. At 300 K the spectra display a broadened doublet with an isomer shift of 0.32 mm.s^{-1} and quadrupolar splitting of 0.71 mm s^{-1}, which corresponds to high-spin Fe(III) ions. The spectrum at 4 K was fitted with two sextets, with isomer shifts of 0.48(5) and 0.46(5) mm s^{-1}, quadrupolar splitting=0.02(1) mm s^{-1}, and magnetic hyperfine field (H_{hf})=50.2 and 48.4 T, typical hyperfine parameters of maghemite in this temperature [10]. These results confirm that the sample is composed mainly of maghemite (γ-Fe_2O_3). Fig. 3 presents a typical high resolution TEM image of the γ-Fe_2O_3 nanoparticles. The average nanoparticle diameter is (3.9 ± 0.5) nm, a fit to the distribution of sizes by a lognormal function gives Dc=4.0 nm and σ=0.1 (see Fig. S1, supplementary information), which is considered as a narrow size distribution. HRTEM images demonstrate that the nanoparticles are both crystalline and faceted. The nanoparticles presented an interlayer d spacing of 0.25 nm, which is expected from main reflective

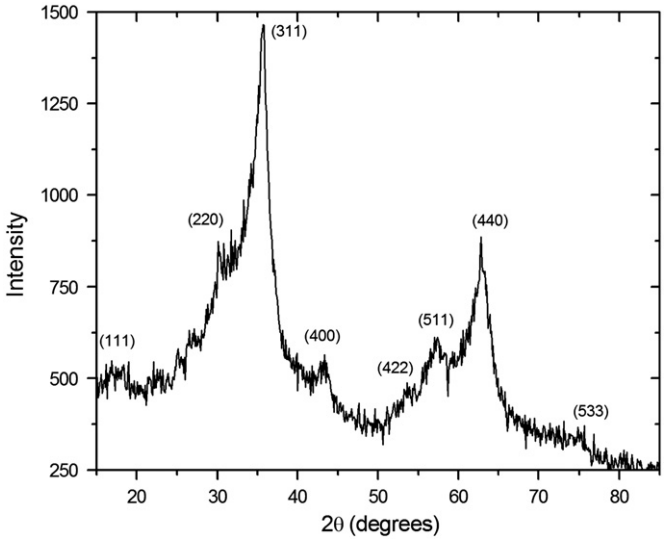

Fig. 1. XRD pattern of γ-Fe_2O_3 nanoparticles.

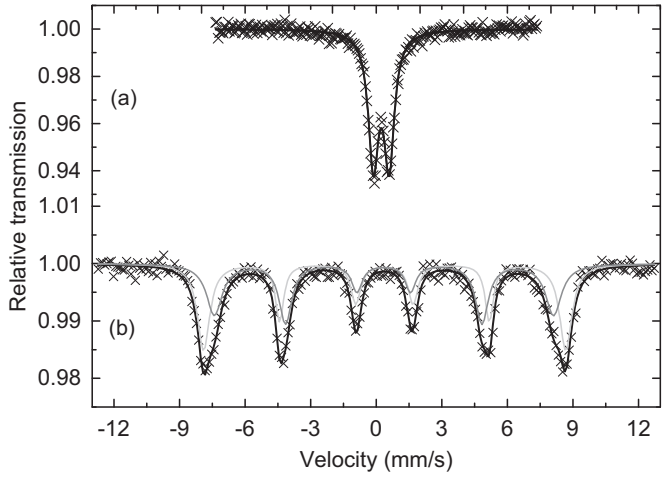

Fig. 2. Mössbauer spectra of γ-Fe_2O_3 nanoparticles at 300 K (a) and 4 K (b) and the best fit shown as the darker line.

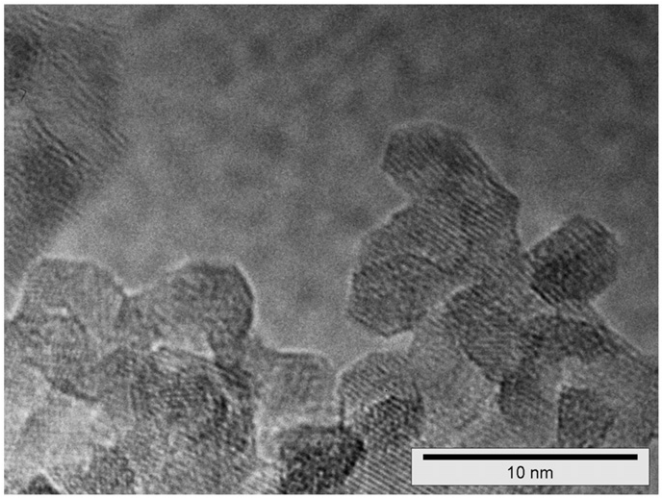

Fig. 3. HRTEM image of γ-Fe_2O_3 nanoparticles.

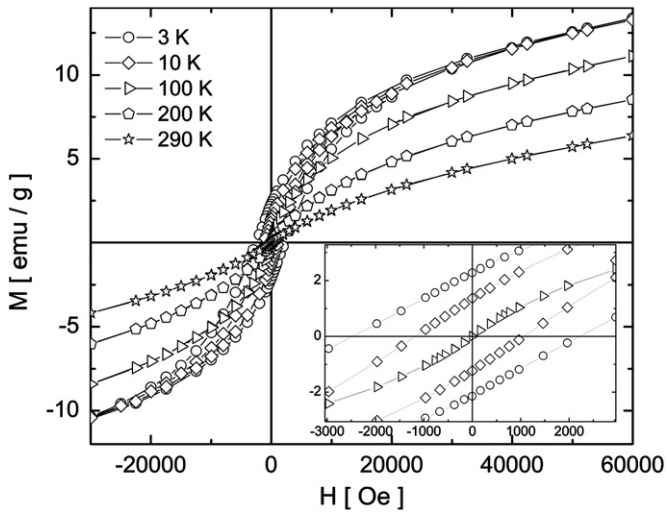

Fig. 4. Isothermal magnetization measurements showing in detail the hysteresis for temperatures below T_B.

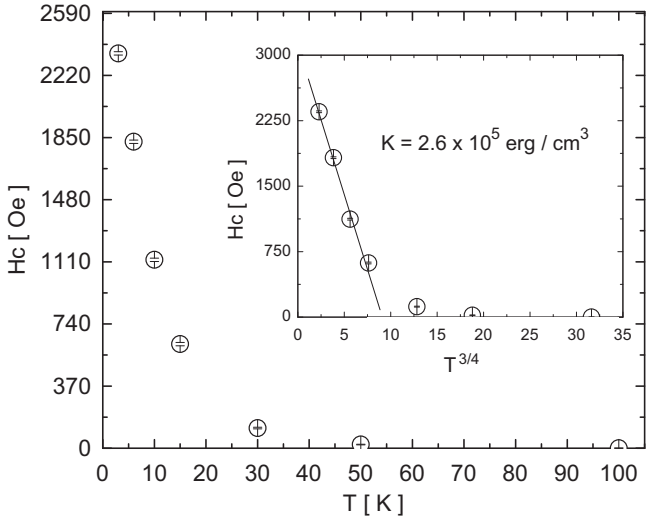

Fig. 5. Temperature dependence of the coercivity obtained from the hysteresis curves.

(311) plane of maghemite. The distribution and other selected TEM image are available as Supplementary Information.

Hysteresis curves measured from 3 K up to 290 K are shown in Fig. 4. The coercivity and the remanence decrease with increasing temperature and are negligible above 100 K. The magnetization does not saturate even at 60 kOe and 3 K, a feature already observed in systems of small maghemite nanoparticles [11]. Mössbauer spectroscopy measurements [12] and Monte Carlo simulations [13] indicate that this effect comes from canting of disordered spin on the surface of the nanoparticles. The surface spin layer reduces the nanoparticles spontaneous magnetization and leads to an apparent additional anisotropy on the high field approach to saturation. A rough estimate of the effective uniaxial anisotropy constant value for our system was obtained from the temperature dependence of coercive field shown in Fig. 5. By neglecting interparticle interaction and their size distribution (thus the superparamagnetic fraction), the coercive field H_C relates to the temperature T [14] as,

$$H_C = 0.5(2K/M_S)[1-(T/\langle T_B\rangle)^{3/4}] \quad (1)$$

where K is the uniaxial magnetic anisotropy constant and M_S is the spontaneous magnetization. According to Eq. (1), H_C is expected to be a linear function of $T^{3/4}$ and K/M_S can be obtained by extrapolation to $T=0$. We can observe that this linear relationship is obeyed only below 8 K, where most of the nanoparticles are blocked. The deviation at higher temperatures is due to the neglected interactions and/or larger size nanoparticles [15]. We used the saturation magnetization as an approximation to the spontaneous magnetizations by extrapolating $M \times 1/H$ to infinite field value at 3 K, finding a value of 17 emu/g, in good agreement with the reported by Morales et al. [16]. Our estimate for the effective anisotropy constant gives a value $K=2.6\times10^5$ erg/cm^3. Note that there is a large spread of M_S and K values in the literature, Fiorani et al. [17] found for maghemite nanoparticles ranging from 2.7 to 8.7 nm, $K=2.5\times10^6$ erg/cm^3 to 4.7×10^5 erg/cm^3 from the irreversibility field (H_{irr}) of hysteresis loops. A recent result found an effective value of $K=2\times10^6$ erg/cm^3 [18].

Our estimate using Eq. (1) gives a lower bound for K as the measured H_C is lowered by neglecting the fraction of superparamagnetic nanoparticles of the sample. We also neglected the effect of the dipolar interactions. Another way to estimate K avoiding the dipolar interactions is following Ref. [17] where $K_{eff}=1/2M_SH_{irr}$. Using the 3 K magnetization loop, $H_{irr}=40$ kOe giving $K=1.7\times10^6$ erg/cm^3. This value is an upper bound for K as it reflects the irreversibility of the nanoparticles with the largest anisotropy energy barrier. An average value between these two extremes would be the most representative value for our sample, so in what follows we will consider $K_{eff}=1\times10^6$ erg/cm^3.

The ZFC/FC curves measured with a field of 100 Oe are shown in Fig. 6(a). ZFC curves were obtained by cooling the sample under zero applied field to 2 K, then applying the desired field and measuring while slowly warming the sample to 300 K. The temperature at the maximum of the ZFC curve is proportional to the average blocking temperature of the particles. Actually, there is a distribution of blocking temperatures (reflecting the size distribution) which can be determined [19] by the derivative of the difference of these curves with respect to temperature, i.e., $d[\chi_{ZFC}-\chi_{FC}]/dT$, see Fig. 6(b). Normalizing and integrating the product of the derivative by the temperature we obtain the average blocking temperature of the system $\langle T_B\rangle=28$ K. The volume is correlated to the blocking temperature ($\langle T_B\rangle$) by:

$$V_C = (25k_BT_B/K) = 4/3(\pi r^3) \quad (2)$$

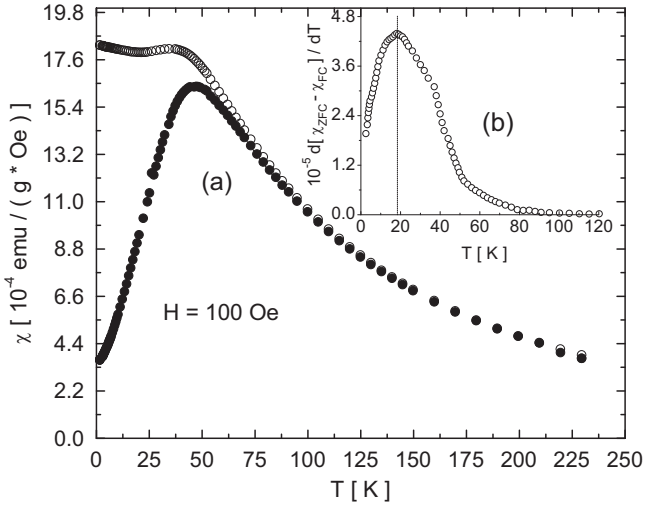

Fig. 6. (a) *ZFC* (●) and *FC* (○) magnetization curves measured under 100 Oe; (b) d[*ZFC*–*FC*]/d*T* representing the distribution of blocking temperature of the nanoparticles.

where k_B is the Boltzmann constant and K is the uniaxial anisotropy constant of the magnetic particles. Using the estimated effective anisotropy constant $K_{eff}=1\times10^6$ erg/cm^3, the average magnetic diameter of the nanoparticles is 5.7 nm.

The difference between the magnetic size and the TEM size is observed in many similar systems and is usually attributed to enhanced anisotropy and interparticle dipolar interaction [20]. Interparticle interactions can also be noted in the field dependence of the mean blocking temperature determined from ZFC/FC data obtained at different fields shown in Fig. 7. Neglecting interparticles interactions and the random orientations of the anisotropy axis, $\langle T_B\rangle$ is related to the field H as [21,22]:

$$\langle T_B\rangle = K\langle V\rangle[1-(H/H_K)]^2/k_B\ln(\tau_{obs}/\tau_0) \quad (3)$$

where $H_K=2$ K/M_S is the anisotropy field, τ_{obs} is the measurement observation time ($\sim$100 s) and τ_0 is a characteristic time of the order of 10^{-9}–10^{-12} s. A clear deviation from the behavior predicted by Eq. (3) is observed around 200 Oe. This is typically found in systems of interacting nanoparticles [22].

Dipolar interactions have a strong influence in the dynamic magnetic response [13] of nanosized systems. This can be overcome by the application of an external DC field, higher than the typical internal dipolar fields. We thus performed AC susceptibility measurements in zero field and in the presence of an applied static field. In Fig. 8 we present the results obtained with $H_{DC}=0$ and $H_{DC}=1$ kOe. Both the in-phase χ' and the out-of-phase χ'' components show a frequency dependent maximum typical of interacting magnetic nanoparticles. When the size distribution is very narrow and interparticle interactions can be neglected, τ is exponentially related to the temperature, $\tau=\tau_0\exp(\Delta E/k_BT)$, and a linear relationship between $\log\tau$ and $1/T$ is observed. From the maximum of χ'' we extracted the relaxation time temperature dependence (see SI—Figs. S2 and S3), shown in Fig. 9 as an Arrhenius plot. Though our data follows a straight line, the extrapolated value of τ_0 in $H_{DC}=0$ is very small, $(1\pm6)\times10^{-43}$ s, which has no physical meaning. The value of the effective energy barrier, $\Delta E/k_B=(38\pm3)\times10^2$ K, is one order of magnitude higher than the ones typically found in systems of isolated particles of the order of $25\langle T_B\rangle$. These values show that the zero field energy barrier is strongly influenced by interparticles interactions.

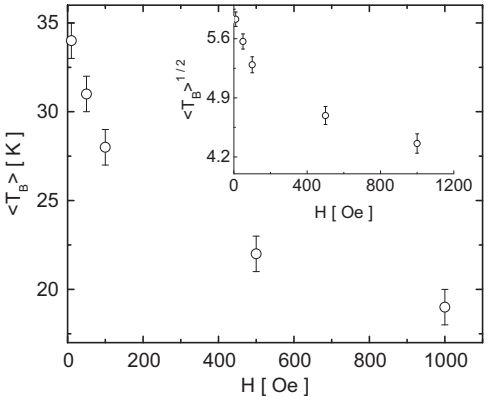

Fig. 7. $\langle T_B\rangle$ and $T_B^{1/2}$ (inset) as a function of the magnetic field. The behavior predicted by Eq. (2) is not observed.

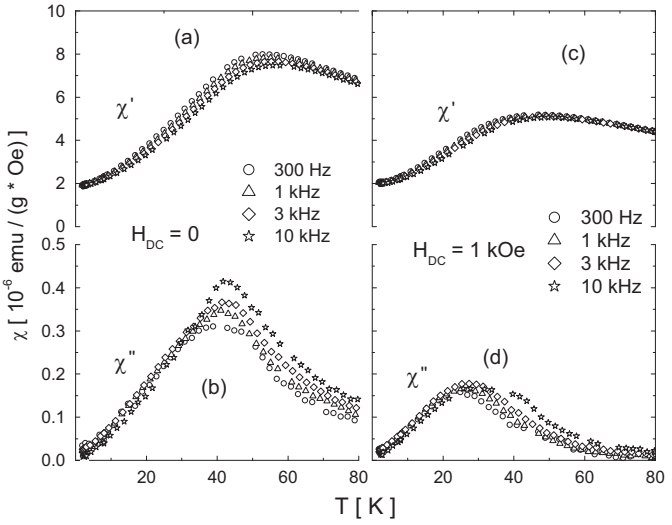

Fig. 8. (a) and (b) In-phase and out-phase components of the AC susceptibility in $H_{DC}=0$. (c) and (d) In-phase and out-phase components of the AC susceptibility in $H_{DC}=1$ kOe.

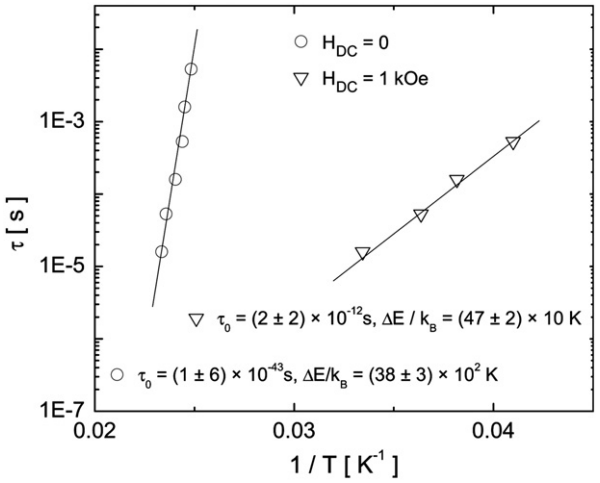

Fig. 9. Arrhenius plot of the dynamic susceptibility in $H_{DC}=0$ (○) and $H_{DC}=1$ kOe (▽).

The measurements made with $H_{DC}=1$ kOe show similar behavior but with different fitting parameters. The obtained value for τ_0 is $(2\pm2)\times10^{-12}$ s, of the order of magnitude expected for isolated nanoparticles. The effective energy barrier, $\Delta E/k_B=(47\pm2)\times10$ K, is one order of magnitude lower than the one found in $H_{DC}=0$. Assuming $\Delta E/k_B=25\langle T_B\rangle$ we found $\langle T_B\rangle\sim19$ K, a value which is in good agreement with the mean blocking temperature in the ZFC and FC susceptibilities measured in 1 kOe, shown in Fig. 8. The fact that the AC susceptibility results under field restore the expected behavior of isolated nanoparticles indicates that 1 kOe is high enough to overcome the internal dipolar field among the particles. This field can be estimated from the dipolar field of one nanoparticle on an identical neighbor by $H_{dip}=M_SV/d^3$. Using the extrapolated value for M_S and the mean diameter from TEM images we found $H_{dip}\sim44$ Oe, which is much smaller than 1 kOe. Finally we compare these results with an estimate of the anisotropy energy barrier ($\Delta E/k_B=KV/k_B$) expected for nanoparticles with mean diameter of 3.9 nm and the estimated anisotropy constant ($K=1\times10^6$ erg/cm^3). We found the value 225 K, which is lower than the dynamic value 470 K, again in agreement with the hypothesis that the energy barrier is enhanced by surface anisotropy contributions.

4. Conclusions

Crystalline maghemite nanoparticles with narrow size distribution were obtained by a new method. From the temperature dependence of the coercivity and the saturation magnetization we estimated the anisotropy constant $K=2.6\times10^5$ erg/cm^3. From low

field ZFC/FC magnetization measurements data we found that the average blocking temperature field dependence was typical of interacting nanoparticles. These magnetic measurements led to an estimated average diameter of 5.7 nm. This value is larger than the values obtained from powder X-ray diffraction (3.0 nm) and also direct observation of the sizes by HRTEM (3.9 nm). These results follow the general understanding that the surface contribution to the anisotropy is relatively larger than in the bulk. We also studied the dynamic behavior of the nanoparticles by AC susceptibility. The obtained relaxation times follow an Arrhenius law with unphysical small values of the τ_0 parameter and too large energy barrier values. Reasonable parameters are recovered when the measurements were done within a static field of 1 kOe, which overcomes interparticle dipolar interactions, leading to a good agreement with estimated parameters from the DC measurements. The large difference between the dynamic energy barrier and the estimated energy barrier from static measurements and TEM sizes is an evidence that the surface contribution to the anisotropy is very large.

Acknowledgment

Financial support was received from CAPES, FAPERJ, FAPEMIG and CNPq (Brazil). M.G. acknowledges a fellowship from CONICET. H.E.T. is a member of CONICET. The authors also acknowledge the LDRX-UFF.

Appendix A. Supplementary material

Supplementary data associated with this article can be found in the online version at http://dx.doi.org/10.1016/j.jmmm.2012.04.049.

References

[1] R. Zboril, A. Bakandritsos, M. Mashlan, V. Tzitzios, P. Dallas, C. Trapalis, D. Petridis, One-step solid state synthesis of capped γ-Fe_2O_3 nanocrystallites, Nanotechnology 19 (2008) 1–8.
[2] S. Laurent, D. Forge, M. Port, A. Roch, C. Robic, L. van der Elst, R. Muller, Magnetic iron oxide nanoparticles: synthesis, stabilization, vectorization, physicochemical characterizations, and biomedical applications, Chemical Reviews 108 (2008) 2064–2110.
[3] T. Hyeon, Chemical synthesis of magnetic nanoparticles, Chemical Communications 8 (2003) 927–934.
[4] A. Dei, D. Gatteschi, C. Sangregorio, L. Sorace, M.G.F. Vaz, Bonding coordination requirements induce a antiferromagnetic coupling between m-phenylene bridged o-iminosemiquinonato diradicals, Inorganic Chemistry 42 (2003) 1701–1706.
[5] S. Lee, J. Jeong, S. Shin, J. Kim, Synthesis and characterization of superparamagnetic maghemite nanoparticles prepared by coprecipitation technique, Journal of Magnetism and Magnetic Materials 282 (2004) 147–150.
[6] E. Delahaye, V. Escax, N. Hassan, A. Davidson, R. Aquino, V. Dupuis, R. Persynski, Y. Raikher, Nanocasting: using SBA-15 silicas as hard templates to obtain ultrasmall monodispersed γ-Fe_2O_3 nanoparticles, Journal of Physical Chemistry B 110 (2006) 26001–26011.
[7] Z. Liu, H.B. Wang, Q.H. Lua, G.H. Du, L. Peng, Y.Q. Du, S. Zhang, K. Yao, Synthesis and characterization of ultrafine well-dispersed magnetic nanoparticles, Journal of Magnetism and Magnetic Materials 283 (2004) 258–262.
[8] J. Wu, S.P. Ko, H. Liu, S. Kim, J. Ju, Y.K. Kim, Sub 5 nm magnetite nanoparticles, Materials Letters 61 (2007) 3124–3129.
[9] A. Dei, D. Gatteschi, C. Sangregorio, L. Sorace, M.G.F. Vaz, HF-EPR to monitor electron transfer in mixed valence dioxolene metal complexes, Chemical Physics Letters 368 (2003) 162–167.
[10] O. Helgason, H.K. Rasmussen, S. MØrup, Spin-canting and transverse relaxation in maghemite nanoparticles and in tin-doped maghemite, Journal of Magnetism and Magnetic Materials 302 (2006) 413–420.
[11] B. Martnez, X. Obradors, L. Balcells, A. Rouanet, C. Monty, Low temperature surface spin-glass transition in γ-Fe_2O_3 nanoparticles, Physical Review Letters 80 (1998) 181–184.
[12] J. Coey, Noncollinear spin arrangement in ultrafine ferrimagnetic crystallites, Physical Review Letters 27 (1971) 1970–1972.
[13] O. Iglesias, A. Labarta, Finite-size and surface effects in maghemite nanoparticles: Monte Carlo simulations, Physical Review B, APS 63 (2001) 184416.
[14] J. Garcıa-Otero, A. Garcıa-Bastida, J. Rivas, Influence of temperature on the coercive field of noninteracting fine magnetic particles, Journal of Magnetism and Magnetic Materials 189 (1998) 377–383.
[15] W.C. Nunes, W.S.D. Folly, J.P. Sinnecker, M.A. Novak, Temperature dependence of the coercive field in single-domain particle systems, Physical Review B 70 (2004) 014419.
[16] M.P. Morales, S. Veintemillas-Verdaguer, M.I. Montero, C.J. Serna, Surface and internal spin canting in γ-Fe_2O_3 nanoparticles, Chemistry of Materials 11 (1999) 3058–3064.
[17] D. Fiorani, A.M. Testa, F. Lucari, F. D'Orazio, H. Romero, Magnetic properties of maghemite nanoparticle systems: surface anisotropy and interparticle interaction effects, Physica B 320 (2002) 122–126.
[19] H. Mamiy, M. Ohnuma, I. Nakatani, T. Furubayashim, Extraction of blocking temperature distribution from zero-field-cooled and field-cooled magnetization curves, IEEE Transactions on Magnetics 41 (2005) 3394–3396.
[20] J. Dormann, D. Fiorani, E. Tronc, Magnetic relaxation in fine-particle systems, Advances in Chemical Physics 98 (1997) 283–494.
[21] Y.D. Zhang, J.I. Budnick, W.A. Hines, C.L. Chien, J.Q. Xiao, Effect of magnetic field on the superparamagnetic relaxation in granular Co–Ag samples, Applied Physics Letters 72 (1998) 2053–2055.
[22] W. Nunes, L. Socolovsky, J. Denardin, F. Cebollada, A. Brandl, M. Knobel, Role of magnetic interpaticle coupling on the field dependence of the superparamagnetic relaxation time, Physical Review B 72 (2005) 1–4.